frontiers | Frontiers in Marine Science

TYPE Original Research
PUBLISHED 07 December 2022
DOI 10.3389/fmars.2022.1075832

OPEN ACCESS

EDITED BY
Abdelfatah Abomohra,
University of Hamburg, Germany

REVIEWED BY
Masoud Salavati-Niasari,
University of Kashan, Iran
Amit Kumar,
Sathyabama Institute of Science and Technology, India

*CORRESPONDENCE
Hana Sonbol
Hssonbol@pnu.edu.sa

SPECIALTY SECTION
This article was submitted to Marine Biotechnology and Bioproducts, a section of the journal Frontiers in Marine Science

RECEIVED 21 October 2022
ACCEPTED 21 November 2022
PUBLISHED 07 December 2022

CITATION
Kamal M, Abdel-Raouf N, Sonbol H, Abdel-Tawab H, Abdelhameed MS, Hammouda O and Elsayed KNM (2022) *In vitro* assessment of antimicrobial, anti-inflammatory, and schistolarvicidal activity of macroalgae-based gold nanoparticles. *Front. Mar. Sci.* 9:1075832. doi: 10.3389/fmars.2022.1075832

In vitro assessment of antimicrobial, anti-inflammatory, and schistolarvicidal activity of macroalgae-based gold nanoparticles

Marwa Kamal[1], Neveen Abdel-Raouf[1,2], Hana Sonbol[3]*, Heba Abdel-Tawab[4], Mohamed Sayed Abdelhameed[1], Ola Hammouda[1] and Khaled N. M. Elsayed[1]

[1]Botany and Microbiology Department, Faculty of Science, Beni-Suef University, Beni-Suef, Egypt, [2]Department of Biology, College of Science and Humanities in Al-Kharj, Prince Sattam bin Abdulaziz University, Al-Kharj, Saudi Arabia, [3]Department of Biology, College of Science, Princess Nourah bint Abdulrahman University, Riyadh, Saudi Arabia, [4]Zoology Department, Faculty of Science, Beni-Suef University, Beni-Suef, Egypt

There is a growing need to improve facile, eco-friendly, and cheap approaches for nanoparticle (NP) synthesis. Green protocols have been investigated for the fabrication of NPs using several natural sources as plants, algae, fungi, and bacteria. Thus, the present study proposed a rapid, convenient, and efficient biosynthesis of gold NPs (Au-NPs) using the ethanolic extracts of three macroalgae, i.e., *Cystoseira myrica, C. trinodis*, and *Caulerpa prolifera*. The reduction of Au ions and the fabrication of Au-NPs were validated using ultraviolet-visible (UV–Vis) spectroscopy, X-ray diffraction, Fourier transform infrared spectroscopy (FT-IR), transmission electron microscopy (TEM), and zeta potential analysis. The produced Au-NPs were tested for their antibacterial, antifungal, anti-inflammatory, and schistolarvicidal activity. Results revealed the formation of Au-NPs with an average size of 12.6–15.5 nm and different shapes that are mainly spherical with pure crystalline nature. The strong antibacterial activities of *C. trinodis*– and *C. myrica*–based Au-NPs against *E. coli* (inhibition zones of 22 and 19 mm) and *against Staphylococcus aureus* (inhibition zones of 18 and 20.5 and mm) were recorded, respectively. On the other hand, the high antifungal activity of *C. trinodis* Au-NPs against *Aspergillus niger and Alternaria alternate* showed the inhibition zones of 18 and 17 mm, respectively. The high antifungal activity of *C. trinodis* Au-NPs against *Candida albicans* (inhibition zone 16 mm) was also recorded. Regarding anti-inflammatory and schistolarvicidal activity, Au-NPs fabricated using *C. myrica* showed 64.2% of the inhibitory effect on protein denaturation and recorded the highest schistolarvicidal activity against *Schistosoma mansoni* cercariae that sank and died after 7 min. Overall, these findings proved that macroalgal

ethanolic extracts can be effectively used for the biosynthesis of Au-NPs. These Au-NPs offer a significant alternative antimicrobial, anti-inflammatory, and schistolarvicidal agents. for biomedical uses.

KEYWORDS

biosynthesized gold nanoparticles, macroalgae, *cystosiera myrica*, *cystosiera trinodis*, *caulerpa prolifera*, antimicrobial, anti-inflammatory, schistolarvicidal

Introduction

Nanotechnology means synthesizing materials at the nanosize that range from 1 to 100 nm (Salem and Fouda, 2021). Nanoparticles (NPs) are widely used in every branch of sciences, including space, industry, defense, communication, biomedicine, agriculture, electronics sectors, energy, and environmental remediation (Salavati-Niasari et al., 2005; Roy et al., 2019: Chaudhary et al., 2020: Heydariyan et al., 2022; Monsef and Salavati-Niasari, 2023). This high interest in NPs is attributed to their distinctive morphological (shape, size, and charge distribution), special physical and chemical properties including a high surface-to-volume ratio, unique optical, magnetic, electronic, and catalytic properties; surface plasmon resonance; and fluorescence emission (Rajeshkumar et al., 2013; Ramakrishna et al., 2016; Borse et al., 2020). There are two methods for NP production, i.e., top–down and bottom–up (Shukla et al., 2021). In the first approach, different mechanisms can be used to slice bulk materials to nanoscale particle sizes, such as evaporation–condensation, laser ablation, or other physical methods. Meanwhile, in the second method, atoms are combined to form the molecular structures of NP size (Khanna et al., 2019; Salem and Fouda, 2021). The bottom–up approach is commonly used for nanoparticle synthesis by chemical methods such as sol–gel technology, coprecipitation, redox processes, and pyrolysis and biological methods using fungi, plants, yeast, bacteria, and viruses (Abdel-Raouf et al., 2017; Hu et al., 2020; Ahmed et al., 2022). However, the synthesis of nanoparticles using conventional chemical and physical methods has many disadvantages such as their toxicity to humans and the environment, the high cost of nanoparticle production (Menon et al., 2017; Wibowo et al., 2019), the low rates of material transformation, and a high energy requirement (Ghosh et al., 2012). Therefore, there is considerable interest in developing eco-friendly and sustainable technologies to produce nanoparticles (Aboelfetoh et al., 2017). To this end, researchers are focused on the green synthesis of biocompatible and eco-friendly NPs because they are safe, highly tunable, cheap, clean, and easily scaled up (Salem and Fouda, 2021; Amin et al., 2021). In this context, natural ingredients like the extracts of higher plants, and macro- and microorganisms are used without adding external reducing, capping, and stabilizing agents. This is because the constituents of these extracts act as effective reducing and stabilizing agents during the production process of NPs (Ramakrishna et al., 2016; Usman et al., 2019; Yassin et al., 2021). The biosynthesis of NPs is differentiated into intracellular and extracellular according to the position of generated NPs (Öztürk, 2019). Intracellular NP synthesis represents the synthesis of NPs that occurs inside the cells. In contrast, extracellular NP synthesis occurs outside of the cell that assist by various exudates such as primary and secondary metabolites including non-protein compounds like nucleic acid, lipids, and antioxidants (Shukla et al., 2021). In this regard, the extracellular formation of NPs is a preferable method because the NP production rate is high and they are easily purified (Pantidos and Horsfall, 2014).

Marine macroalgae (seaweeds) represent a diverse group of large multicellular eukaryotic photosynthetic organisms. They are found on coastal water areas up to 180 m depth attached to several types of substrates, such as rocks, plants, and dead corals (Faradilla et al., 2022). Marine macroalgae are rich in secondary metabolites such as carotenoids (carotene and xanthophyll) and phycobilins (phycocyanin and phycoerythrin) (Elsayed et al., 2017a; Elsayed et al., 2017b; Fawcett et al., 2017; Pereira, 2018; Fathy et al 2021) and secondary metabolites that empower macroalgae to act as nanobiofactories for metallic NP production (Khanna et al., 2019). This indeed increases the ability to reduce, cap, and stabilize the metal precursors to form metal, metal oxide, or bimetallic NPs (Chaudhary et al., 2020). Furthermore, the biosynthesis of NPs using algae is valuable and attractive because algae have many advantages such as high metal absorption, low cost, non-toxicity, and easy availability (Soureshjani et al., 2021). Many studies proved the ability of several marine algae to generate different metallic NPs (Aboelfetoh et al., 2017; El-Kassas and Ghobrial, 2017; Fawcett et al., 2017; González-Ballesteros et al., 2017; Manikandakrishnan et al., 2019; Babu et al., 2020). NP-based macroalgae were studied for their biomedical applications, which include antibacterial, antifungal, antioxidant, anticancer, antifouling, bioremediation, and biosensing activities (Mayer et al., 2013; Khanna et al., 2019;

Chaudhary et al., 2020; González-Ballesteros et al., 2020; Hu et al., 2020; Gomathy et al., 2021). Among the metallic NPs, Gold nanoparticles (Au-NPs) are the most potent (Pulakkat and Patravale, 2020) due to the unique and tunable surface plasmon resonance, and electrical conductivity and perfect catalytic activity (Tao, 2018). Au-NPs have the overgrown potential for various agriculture and biomedical applications, including drug delivery, molecular imaging, biosensing, and biodiagnostic applications (Sahoo et al., 2014; Khandelia et al., 2015; Khan et al., 2019).

Nowadays, it is necessary to discover or improve compounds with an antimicrobial action because of the increase in microbial infection rates, the rapid development of antibiotic resistance, and the quick evolution of bacteria due to mutation (González-Ballesteros et al., 2020). The use of metal NPs as novel antimicrobial agents is considered as a viable solution for limiting or inhibiting the growth of many pathogenic species (Abdel-Raouf et al., 2017). Another biomedical importance of NPs is their antiparasitic activity against many parasites causing human diseases. Thus, NPs offer a significant antiparasitic effect directly or through working as a vehicle for conventional drugs used for treatment (Moustafa et al., 2018). One of most epidemic neglected tropical diseases (NTDs) in sub-Saharan Africa is schistosomiasis (Adekiya et al., 2017). Schistosomiasis is a water-based debilitating illness induced by blood fukes of the genus *Schistosoma* (Colley et al., 2014). Globally, it is endemic in more than 70 countries and affects around 240 million individuals (Barry et al., 2013). It is a major health problem and a main source of morbidity and mortality worldwide (Elfaki et al., 2020). Widely, *Schistosoma mansoni* is the most prevalent parasite causing intestinal schistosomiasis (WHO, 2015). The infection happens once the host's skin is penetrated by the cercaria, the free-swimming larval stage of schistosomes released by the intermediate host snail (Hotez et al., 2014). Once inside the host, they transform into schistosomula, mature and form couples in the venous system. There are two major forms of schistosomiasis (intestinal and urogenital) with the intestinal schistosomiasis caused by *S. mansoni* being the most prevalent one (WHO, 2015). A novel schistolarvicidal agent needs to be explored and developed urgently to prevent schistosomiasis. *Cystoseira myrica, C. trinodis*, and *Caulerpa prolifera* were chosen for this study because they are dominant species along the Red sea shores of El Quoseir and Marsa Allam which are abundant in all seasons of the year.

According to our knowledge, the biosynthesis of Au-NPs using marine macroalgae *C. trinodis* and *C. prolifera* ethanolic extracts are scarcely studied. Therefore, the present study aims to biosynthesize Au-NPs using ethanolic extracts from three marine macroalgae i.e., *C. myrica, C. trinodis*, and *C. prolifera* to investigate their ability to act as reducing and capping agent for the biosynthesis of Au-NPs. Different physicochemical properties of fabricated Au-NPs were characterized using UV–Vis, XRD, FT-IR, TEM, and zeta potential analysis. Finally, the antimicrobial (antibacterial and antifungal), anti-inflammatory, and schistolarvicidal activities of Au-NPs were evaluated.

Materials and methods

The methods of the biosynthesis, characterization, and biological activities of the produced macroalgae-based Au-NPs are summarized in Figure 1.

Collection, identification, and preparation of macroalgae species

Macroalgal species *C. myrica, C. trinodis*, and *C. prolifera* (Figure 2) were harvested at low tide from El Quoseir (26° 2'34.02" N; 34°18'51.51" E) and Marsa Allam (25°4'11.41"N; 34° 53'56.22"E), Red Sea coast, Egypt. Seaweeds were washed thoroughly with tap and distilled water to remove salt and other impurities. Macroalgal species were morphologically identified at Phycology lab, Botany and Microbiology Department, Faculty of Science, Beni-Suef University, Beni-Suef, Egypt, according to the description of Chapman and Chapman (1980) and Robert (1989). Macroalgal samples were air-dried in the shade for 1 week, and the dried samples were processed in fine powder with a food mixer and stored in labeled sealed vacuum bags for further use (Osman et al., 2020).

Preparation of macroalgae ethanolic extracts

The dried powder of macroalgal species *C. myrica, C. trinodis*, and *C. prolifera* (20 gm) was soaked in 200 ml ethanol (99%) and shaken at room temperature for 24 h. Then, the extract was filtered on Whatman paper no. 1, and the extracts were evaporated in a rotary evaporator at 45°C. The stock solutions (200 mg/ml H_2O) of each algal extract were prepared for further studies (Abdel-Raouf et al., 2017).

Biosynthesis of gold nanoparticles

For the synthesis of Au-NPs using the algal ethanolic extract, 1 ml of the ethanolic extract was added to 99 ml of 10^{-3} M aqueous chloroauric acid ($HAuCl_4$) solution in a 250 ml conical flask and kept at room temperature for 10 min to 12 h) on a magnetic stirrer (120 rpm) in addition to the control (without seaweed extract, only chloroauric acid) was prepared along with the experimental flask (Abdel-Raouf et al., 2017). The formation of Au-NPs was confirmed by changes in the solution color from pale yellow to ruby red or pinkish.

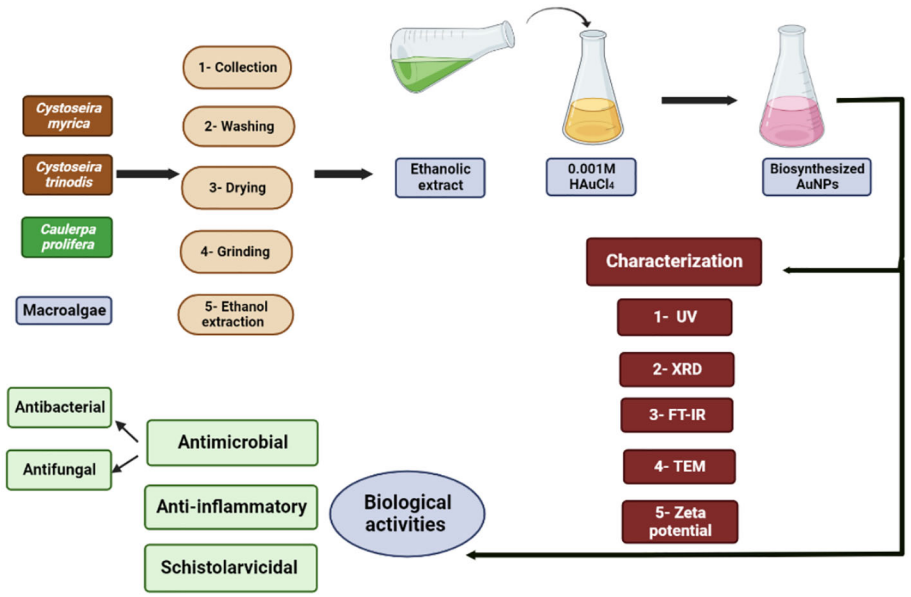

FIGURE 1
Schematic diagram of the experimental methods of the current study.

Characterization of biosynthesized gold nanoparticles

UV–visible spectroscopy analysis

The UV-visible (UV-Vis) diffuse reflectance absorption spectra of Au-NPs were obtained by a UV-VIS-NIR spectrophotometer (T-70) at a wavelength range from 200 to 900 nm.

X-ray diffraction

The X-ray diffraction (XRD) pattern of the prepared material was recorded using PANalytical Empyrean XRD using Cu Kα radiation (wavelength 0.154 cm^{-1}) at an accelerating voltage of 40 kV, a current of 35 mA, a scan angle of the 5°–75° range, and a scan step of 0:02°. The average crystal size was calculated using Debye–Scherrer's equation, shown below (Patterson, 1939).

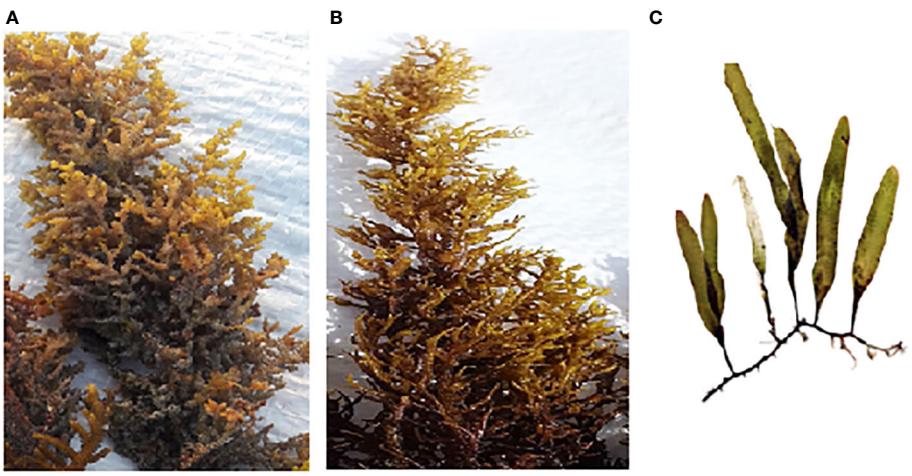

FIGURE 2
Macroalgal species used for the biosynthesis of Au-NPs **(A)** *Cystoseira myrica*, **(B)** *Cystoseira trinodis*, and **(C)** *Caulerpa prolifera*.

$$D = 0.94\,\lambda/\beta\cos\theta,$$

where D is the crystallite size, λ is the X-ray wavelength, β is the broadening of the diffraction peak, and θ is the diffraction angle.

Fourier transform infrared spectroscopy

FT-IR was used to examine the chemical bond vibrations of samples; FT-IR spectra were measured on a Bruker (Vertex 70 FT-IR) spectrometer from 400 to 4,000 cm^{-1}.

Transmission electron microscopy analysis

The morphological analysis of the NPs was done with transmission electron microscopy (TEM). For TEM analysis, a drop of the Au-NP solution was placed on the carbon-coated copper grids, letting the water evaporate till dry at room temperature. Electron micrographs were obtained using a JEOL-1010 transmission electron microscope at 80 kV at the Regional Center for Mycology and Biotechnology (RCMB), Al-Azhar University, Egypt (Amin et al., 2021).

Zeta potential

Zeta potential was measured on a Zeta sizer nano-ZS 90 (Malvern Instruments, UK) at 25°C in clear disposable zeta cells.

Antimicrobial activity of biosynthesized gold nanoparticles

The disk diffusion method was followed to evaluate the antibacterial activity of Au-NPs prepared from different macroalgal ethanolic extracts according to Ramli et al. (2021) against *Staphylococcus aureus* (ATCC 43300), *Listeria monocytogenes* (ATCC 7644), and *Enterococcus faecalis* V853 as Gram-positive pathogenic bacteria and *Escherichia coli* (*E. coli*) (ATCC 25922), *Salmonella enterica* (ATCC 14028) as Gram-negative bacteria. The cultures of these bacteria were obtained from the Faculty of Pharmacy, Beni-Suef University, Beni-Suef, Egypt. These pathogenic bacteria were freshly cultured on nutrient broth for 24 h and then inoculated on nutrient agar. Discs (5 mm) were produced from filter paper Whatman No.1 by using a paper punch, put in a foil packet, and sterilized in the autoclave. Discs were loaded by 5 µl of biosynthesized Au-NPs and ethanolic extracts of the tested macroalgae. Antibacterial activity was detected by measuring the diameter (mm) of inhibition zones around each disc after 24 h incubation at 37°C. Pathogenic fungi *Aspergillus niger* (TUCIM 6581), *Alternaria alternate* (AUMC 5921), and *Fusarium solani* (AUMC 221) as well as the yeast *Candida albicans* (ATCC 60193) were obtained from the Faculty of Sciences, Beni-Suef University, Beni-Suef, Egypt. The antifungal activity of the produced Au-NPs was tested using potato dextrose media. There were 5 mm discs of filter paper Whatman No.1 loaded by 5 µl of biosynthesized Au-NPs; antifungal activity was measured by the diameter (mm) of inhibition zones around each disc after 48 h incubation at 25° C. The chloroauric acid solution was used as the negative control. Ampicillin and fluconazole (100 µg/ml) were used as positive controls to compare the results of antibacterial and antifungal tests, respectively.

Inhibition of albumin denaturation assay

This assay is based on the ability of the substances to inhibit protein denaturation, as described by Elias and Rao (1988). The reaction mixture consisted of 1 ml of the serial concentration of Au(CM)-NPs, Au(CT)-NPs, and Au(CP)-NPs (12.5, 25, 50, 100, and 200 µg/ml) and standard diclofenac sodium with 1.0 ml of a fresh egg-albumin solution and incubated at 27°C ± 1°C for 15 min. Denaturation is induced by keeping the reaction mixture at 70°C in a water bath for 10 min. After cooling down, the turbidity of the sample was measured spectrophotometrically at 660 nm. The inhibition ratio of denaturation was estimated from the blank where no samples were added. Every test was done in triplicate, and the mean was appropriated. The protein denaturation activity was measured using Equation 5:

$$\text{Protein denaturation } \% = A_{(\text{blank})} - A_{(\text{sample})}/A_{(\text{blank})} \times 100$$

Shistolarvicidal activity

S. mansoni cercariae were obtained from experimentally infected *B. alexandrina* snails at 25°C ± 2°C. The snails were obtained from the Schistosome Biological Supply Centre.

Cercaricidal activity

To assess the toxic effect of *C. myrica*, *C. trinodis*, and *C. prolifera* macroalgae–based Au-NPs on the newly formed cercariae, approximately 5 ml of the prepared Au-NPs (200 µg/ml) was added to 100 newly formed cercariae found in 5 ml of water (Ibrahim and Abdel-Tawab, 2020). As a control group, 10 ml of dechlorinated tap water was added to 100 newly formed cercariae. The vitality of cercariae was recorded after 4, 7, 10, 13, 16, 19, 22, 25, and 30 min using the dissecting microscope (Eissa et al., 2011).

Statistical analysis

The data collected were analyzed using the SPSS Statistics software package, version 20 (IBM Corporation, USA).

The Kolmogorov–Smirnov and Levene tests for the homogeneity of variances were applied to check the data for normality and homoscedasticity. Data are expressed as the mean ± SD of three replicates. Differences between treatments were determined by *post-hoc* TukeyHSD (a one-way ANOVA followed by Tukey's test for multiple comparisons of means ($P \leq 0.05$) Significant differences were considered at $p < 0.05$.

Results

In the current study, Au-NPs were biosynthesized using the ethanolic extracts of three macroalgae, brown macroalgae *C. myrica, C. trinodis*, and green macroalgae *C. prolifera* collected from Red Sea, Egypt, and investigated their biological activities such as antimicrobial (antibacterial and antifungal), anti-inflammatory, and schistolarvicidal activities.

Characteristics of the synthesized nanoparticles

Ultraviolet

The complete reduction of Au^{+3} to Au^{0} and the formation of Au-NPs were verified by the change in the color of the solution mixture from pale yellow (the color of chloroauric acid and the macroalgal extract) to a ruby-red or pinkish color that is a characteristic of Au-NPs (Ramakrishna et al., 2016), followed by UV–Vis spectrophotometer analysis. The formation of Au-NPs was indicated by the dominant single-surface plasmon resonance (SPR) peak at 545, 540, and 555 nm of macroalgae *C. myrica, C. trinodis*, and *C. prolifera*, respectively, in the UV–visible spectra as shown in Figures 3A–C.

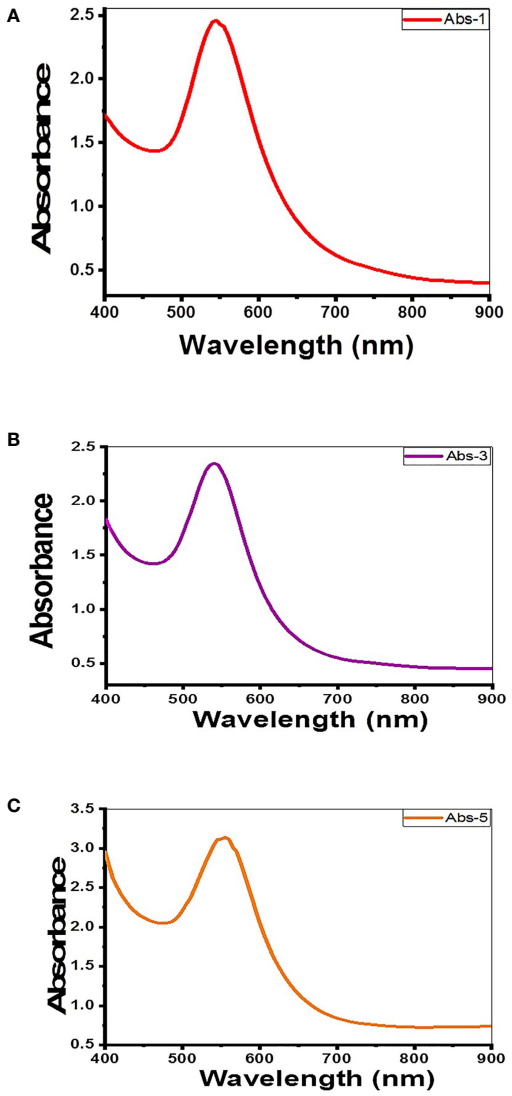

FIGURE 3
UV–visible spectrum of Au-NPs biosynthesized using extracts of macroalgae **(A)** *C. myrica*, **(B)** *C. trinodis*, and **(C)** *C. prolifera*.

X-ray reflective diffraction

X-ray reflective diffraction (XRD) is the primary analytical tool used to identify chemical phases and the crystallite size of the produced Au-NPs in the region of 400–4,000 cm^{-1}.The XRD pattern of Au-NPs synthesized using the *C. myrica* ethanolic extract shows six diffraction peaks at 28.4°, 38.6°, 40.5°, 44.7°, 64.9°, and 77.9°, as noticed in Figure 4A. The crystallite size calculated using Scherrer's equation was approximately 20 nm. The size distribution was presented between 9.5 and 64 nm. Results indicate that the intense diffraction peaks of Au-NPs at 2θ = 38.6°, 44.7°, 64.9°, and 77.9° which matches to (111), (200), (220), and (311) (JCPDS no 04.0784) (Kayalvizhi et al., 2014) lattice planes for the face center cubic structure characterized of Au-NPs. The XRD pattern of Au-NPs of *C. trinodis* is shown in Figure 4B. There were 13 sharp diffraction peaks observed at 28.4°, 31.9°, 33.1°, 38.5°, 40.3°, 44.6°, 45.6°, 49.9°, 57.8°, 64.9°, 65.9°, 73.0°, and 77.9°. Four distinctive peaks were observed at 2θ = 38.5°, 44.6°, 64.9°, and 77.9°, which are indexed as (111), (200), (220), and (311) (JCPDS no 04.0784) (Kayalvizhi et al., 2014) lattice planes denoted the cubic shape of AuNPs. The crystallite size calculated using Scherrer's equation was approximately 41 nm. The size distribution was recorded between 17 and 64 nm. The XRD pattern of *C. prolifera*–based Au-NPs is shown in Figure 4C. There were 13 sharp diffraction intensities observed at 28.3°, 32.1°, 38.4°, 40.4°, 44.7°, 45.7°, 49.8°, 56.7°, 58.3°, 64.9°, 73.1°, 75.5°, and 77.8°. Four distinctive peaks were noticed at 2θ = 38.4°, 44.7°, 64.9°, and 77.8°, which correspond to (111), (200), (220), and (311) (JCPDS no 04.0784) (Kayalvizhi et al., 2014) lattice planes denoted the cubic shape of

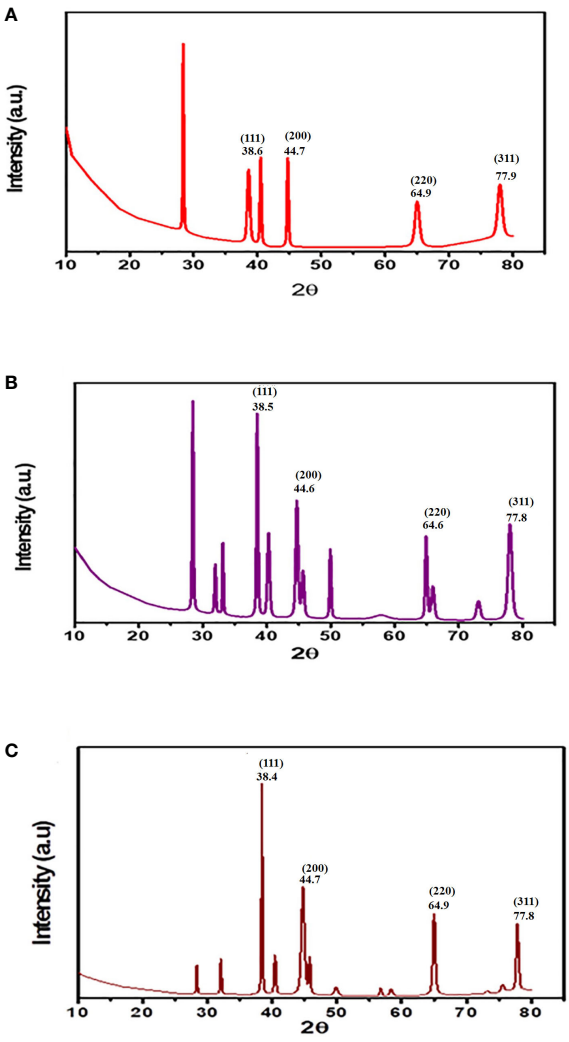

FIGURE 4
XRD pattern of Au-NPs biosynthesized using the ethanolic extracts of macroalgae **(A)** *C. myrica* **(B)** *C. trinodis*, and **(C)** *C. prolifera*.

AuNPs. The crystallite size calculated using Scherrer's equation was approximately 65 nm. The size distribution was recorded between 15 and 65 nm.

Fourier transform infrared analysis

FT-IR spectrum is a tool that supplies information about the structure of the possible biomolecules on the Au-NP surface and predicts functional groups that are involved in the reduction of Au (III) ions and capping of the Au-NPs. The FT-IR spectra of the colloidal solution of Au-NPs biosynthesized using a seaweed ethanolic extract were analyzed in the range between 400 and 4,000 cm^{-1}. The FT-IR spectrum of the Au-NPs of *C. myrica* shows six bands at approximately 3,378.2, 2,931.4, 1,639.6, 1,388.9, 1,076.6, and 613.4 cm^{-1} (Figure 5A). The presence of the band at 3378.168 cm^{-1} may be related to $-NH_2$ and –OH groups (Ghiyasiyan-Arani et al., 2017; Arévalo-Gallegos et al., 2018; Fathy et al., 2020; Hussein et al 2022). This broadness is due to the overlap of both the O–H bond stretching of the high concentrations of alcohols or phenols or polysaccharides and the N–H stretching of 1ry amines (Chandini et al., 2008; Devi et al., 2011). Polysaccharides are rich in brown algae; thus, they have abundant hydroxyl groups. The small band at 2931.4 cm^{-1} may indicate the presence of the (C-H) stretching of alkanes (Panahi-Kalamuei et al., 2015). The small peak observed at 1,639.6 cm^{-1} can be assigned to the stretching vibration of the C=O of free hydroxyl and a carboxylic acid group (Fernández et al., 2011). The sharp band observed at 1,388.9 cm^{-1} may be due to the presence of NO_2 indicated by absorption peaks. The small band at 1,076.6 cm^{-1} may be attributed to the presence of c-o/c-c/c-N stretching vibration. The broad band at 613.4 cm^{-1} could be associated with the C–Cl-stretching vibration of alkyl halides (Bakshi et al., 2008). The FT-IR spectrum of Au-NPs created by brown macroalgae *C. trinodis* exhibited six bands positioned at approximately 3,361.8, 1,641.9, 1,399.4, 1,075.9, 886.1, and 605.5 cm^{-1} (Figure 5B).The broad band observed at 3,361.8 cm^{-1} may be recognized as the stretching vibration of the O-H group of phenols or polysaccharides or alcohol molecules (Bafana, 2013; Arévalo-Gallegos et al., 2018). The presence of two bands positioned at 1,641.9 and 1,399.4 cm^{-1} may be attributed to the asymmetrical and symmetrical stretching of the carboxylate groups from the amide I and II of proteins (Fernández et al., 2011). The band observed at 1,075.9 cm^{-1} may be due to the stretching vibrations of the C-O group of the sugar ring and glycosidic bond (Rajathi et al., 2012). The sharp bands positioned at 886.1 cm^{-1} may be attributed to C-O-S bending vibration, which confirms the presence of sulfate groups in the polysaccharide structure (Alipour et al., 2018). The broad band at 605.5 cm^{-1} may correspond to the C–Cl-stretching vibration of alkyl halides (Bakshi et al., 2008). The FT-IR spectrum of biogenic Au-NPs by the ethanolic extract of *C. prolifera* (Figure 5C) shows the formation of nine bands positioned at approximately 3,366.9, 2,920.1, 2,852.5, 1,705.3, 1,395.6, 1,226.8, 1,050.1, 737.4, and 608.5 cm^{-1}. The broad band observed at approximately 3,366.9 cm^{-1} denoted the O-H stretching vibrations of the hydroxyl group (Gholami et al., 2017) and N-H stretching vibrations, which confirmed the presence of alcohols, amides, and amines, respectively (Babu et al., 2020). Two sharp bands positioned at 2,920.1 and 2,852.5 cm^{-1} may correspond to the (C-H) stretching vibrations of alkanes (Mir and Salavati-Niasari, 2013; Monsef et al., 2018). The band positioned at approximately 1,705.3 cm^{-1} may be due to the stretching of C=O groups (Aboelfetoh et al., 2017). The sharp band at 1,395.6 cm^{-1} may correspond to the asymmetrical stretching vibration of the carboxylate group (Fernández et al., 2011). Two small bands at 1,226.8 and 1,050.1 cm^{-1} were related to the C–N stretching vibration of aliphatic amines (Ramakrishna et al., 2016). Two small absorption bands at 737.4 and 608.5 cm^{-1} may correspond to the presence of the

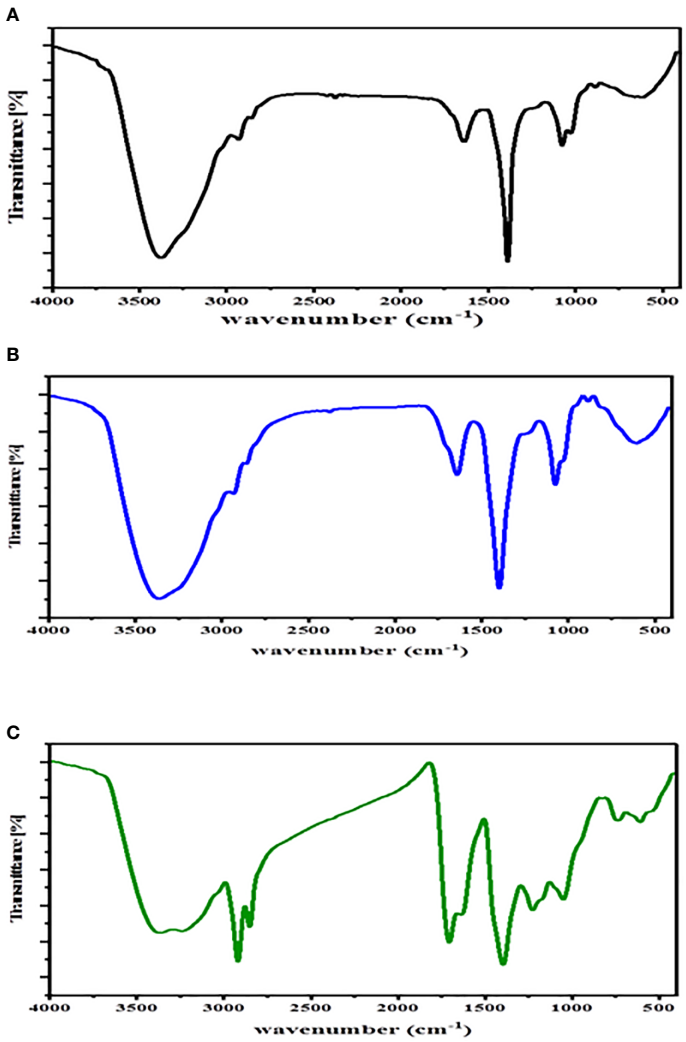

FIGURE 5
FT-IR spectrum of Au-NPs biosynthesized using ethanolic extracts of macroalgae **(A)** *C. myrica*, **(B)** *C. trinodis*, and **(C)** *C. prolifera*.

sugar cycle and C–Cl-stretching vibration of alkyl halides, respectively (Bakshi et al., 2008).

High-resolution transmission electron microscopy

Transmission electron microscopy (TEM) was employed to detect both the size and shape of the synthesized Au-NPs, in addition to illustrating the purity, polydispersity, and surface properties of the produced NPs (Rónavári et al., 2021). The TEM image of Au-NPs synthesized from the extract of macroalgae *C. myrica* (Figure 6A) illustrates that the Au-NPs were varied between spherical and hexagonal in shape and well distributed. They also have diameters ranging from 5.9 to 16.2 nm approximately, with an average size of 12.6 nm ± 3.05 nm. The TEM image of Au-NPs produced using macroalgae *C. trinodis* extract revealed that most of the Au-NPs are nearly spherical in shape with diameters ranging from 9.3 to 22 nm with an average size of 15.5 nm (Figure 6B). The Au-NPs of *C. prolifera*, as shown in Figure 6C, are anisotropic where the Au-NPs varied between spherical, hexagonal, and triangular shapes within a compressed matrix. They have diameters ranging from 8.2 to 20.8 nm with an average size of 14.8 nm ± 3.2 nm.

Zeta potential

Zeta potential is used to determine the amount of the charge repulsion–attraction, which impacts the stability of the Au-NPs (Rónavári et al., 2021). Its determination revealed the causes of material aggregation, coagulation, or flocculation in suspensions.

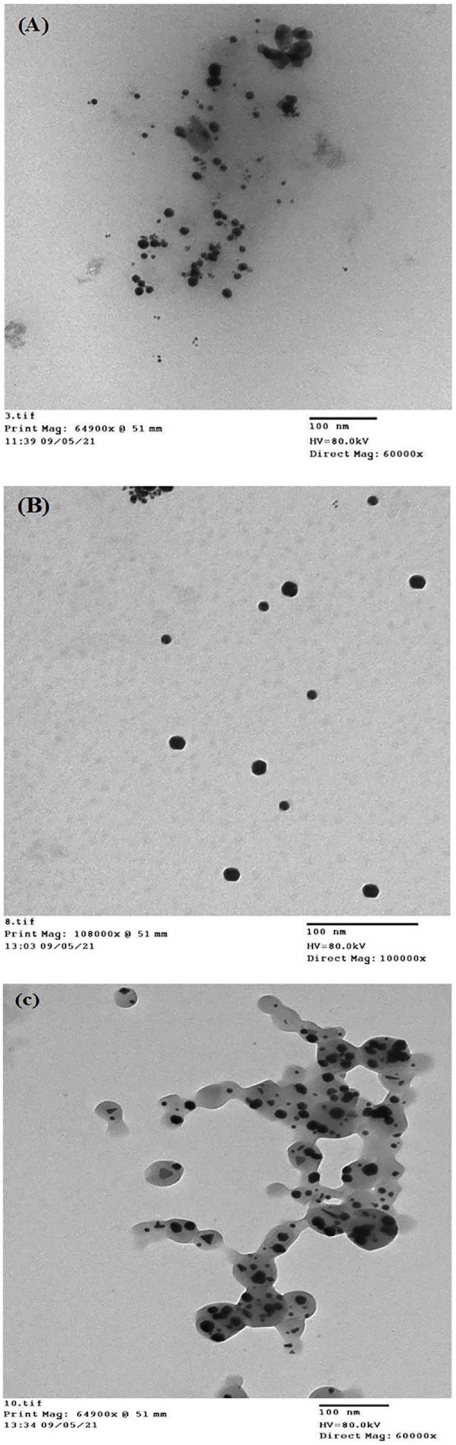

FIGURE 6
TEM micrograph of Au-NPs biosynthesized using the extracts of macroalgae **(A)** *C. myrica*, **(B)** *C. trinodis*, and **(C)** *C. prolifera*.

The zeta potential values of biosynthesized Au-NPs were -20, -40.3, and -47.2 mV for *C. myrica*, *C. trinodis*, and *C. prolifera*, respectively (Figures 7A, B).

Bioactivity of biosynthesized gold nanoparticles

Antimicrobial activity

The biosynthesized Au-NPs showed a variable degree of antimicrobial activities against tested pathogenic microorganisms (Table 1 and Figure 8). For the antibacterial test, maximum inhibition zones against *Escherichia coli* (22 and 19 mm) were exhibited by the Au-NPs of *Cystosiera myrica* and *C. trinodis*, respectively, as well as against *S. aureus* inhibition zones (20.5 and 18 mm) were recorded by Au-NPs using *C. trinodis* and *C. myrica*, respectively. Maximum inhibition zone (17 mm) was formed by Au-NPs of *C. prolifera* against *E. coli* and *S. aureus*, while this it induces minimum inhibition zone (11mm) against *Listeria monocytogenes*. Moreover, ethanolic extracts of the three species of macroalgae exhibited a very weak inhibition zone against all tested microorganisms. For the antifungal test, the maximum inhibition zone (18 mm) was recorded for Au-NPs produced by *C. trinodis* against *Aspergillus niger* followed by inhibition zone (17 mm) for the Au-NPs of *C.myrica* against *Alternaria alternata*. Inhibition zone (16 mm) was recorded by biosynthesized Au-NPs using *C. trinodis* against *C. albicans*. In contrast, the minimum inhibition zone (11mm) was recorded by Au-NPs of *C. myrica* against *C. albicans*. Au-NPs of *C. prolifera* recorded inhibition zone (15 and 14 mm) against *A. alternate* and *A. niger*, respectively. In addition to the inhibition zone (13 mm) against *C. albicans* and *Fusarium solani*.

Anti-inflammatory activity

The effect of macroalgae-based Au-NPs on protein denaturation was analyzed (Figure 9). The inhibition activity of Au-NPs fabricated using *C. myrica* Au(CM)-NPs, *C. trinodis* Au(CT)-NPs, and *C. prolifera* Au(CP)-NPs at 200 µg/ml was 64.2% ± 1.27%, 55.10%, and 52.61%, respectively, while standard diclofenac sodium offered the inhibition of the protein denaturation activity of 66.24% at the same concentration.

Schistolarvicidal activity

The toxic effect of macroalgae-based Au-NPs (Au (CM)-NPs, Au (CP)-NPs, and Au (CT)-NPs) was evaluated against the larval stage of *S. mansoni* (cercariae). Au(CM)-NPs exhibit the most potent cercaricidal activity as 7 min was enough to kill all exposed cercariae (100% mortality) compared to 0% of the

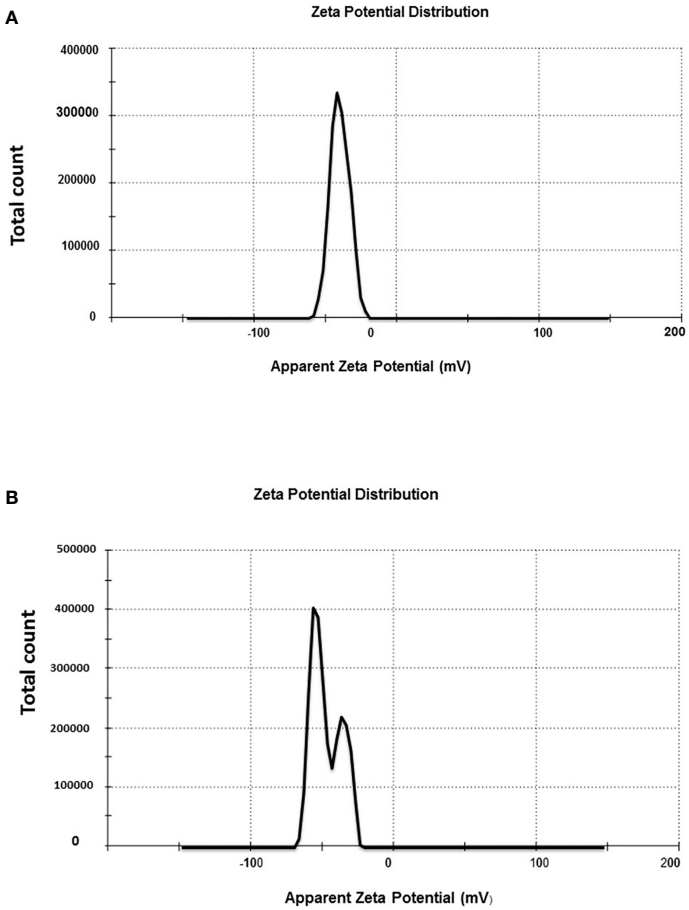

FIGURE 7
Zeta potential distribution of Au-NPs biosynthesized using the extracts of macroalgae **(A)** *C. trinodis* and **(B)** *C. prolifera*.

TABLE 1 Antimicrobial (antibacterial and antifungal) activity of gold nanoparticles biosynthesized using macroalgae *C. myrica, C. trinodis,* and *C. prolifera* against tested pathogenic bacteria and fungi evaluated by the inhibition zone diameter in mm.

Test microorganisms	Diameter of inhibition zone in mm			
	Au-NPs of *C. myrica*	Au-NPs of *C. trinodis*	Au-NPs of *C. prolifera*	Ampicillin or fuconazole
Staphylococcus aureus (ATCC 43300)	18 ± 0.58^{ab}	20.5 ± 0.29^{b}	17 ± 0.58^{a}	17
Listeria monocytogenes (ATCC 7644)	13 ± 0.58^{ab}	14 ± 0.29^{b}	11 ± 0.29^{a}	21
Enterococcus faecalis (V853)	12 ± 0.29^{a}	12 ± 0.58^{a}	15 ± 0.58^{b}	22
Escherichia coli (ATCC 25922)	22 ± 0.58^{c}	19 ± 0.58^{ab}	17 ± 0.58^{bc}	17
Salmonella enterica (ATCC 14028)	16 ± 0.58^{bc}	18 ± 0.58^{c}	13 ± 0.58^{a}	16
Candida albicans (ATCC 60193)	12 ± 0.00^{a}	16 ± 0.58^{b}	13 ± 0.00^{a}	11
Fusarium solani (AUMC 221)	15 ± 0.58^{a}	15 ± 0.00^{a}	13 ± 0.58^{a}	18
Aspergillus niger (TUCIM 6581)	16 ± 0.58^{ab}	18 ± 0.58^{b}	14 ± 0.58^{a}	16
Alternaria alternate (AUMC 5921)	17 ± 0.58^{b}	16 ± 0.58^{ab}	15 ± 0.00^{ab}	25

Different letters mean significant at $p < 0.05$.

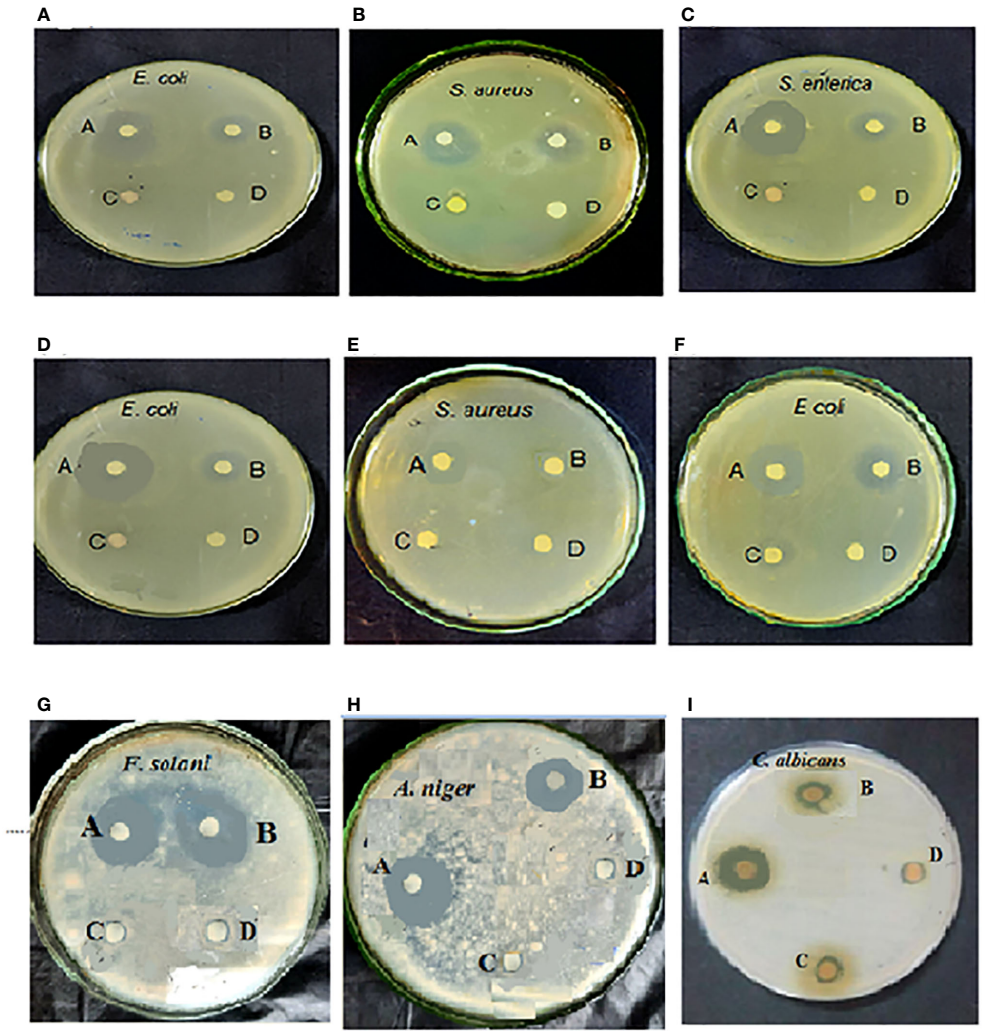

FIGURE 8
Antimicrobial (antibacterial and antifungal) activity of the Au-NPs of *C. trinodis* **(A–C, I)**, *Cystoseira myrica* **(D, E, G, H)**, and *C. prolifera* **(F)**. Letters on the Petri dish: **(A)** Au-NPs, **(B)** ampicillin or fuconazole, **(C)** chloroauric acid, and **(D)** ethanolic extract.

deaths in the control group (Figure 10), followed by Au(CP)-NPs as it achieved 100% mortality after 16 min, while Au(CT)-NPs showed the lowest biocidal effect (100% mortality after 30 min).

Discussion

Recently, the biosynthesis of Au-NPs has been preferred over the chemical and physical fabrication of NPs because of the eco-friendly and non-toxic nature of the produced NPs, as well as high biocompatibility and sensitivity (Purohit et al., 2019). UV–visible spectroscopy is used to demonstrate the production of metal NPs by evaluating the unique optical properties of the NPs, which are dependent on their size and shape (Paulkumar et al., 2017). The formation of this strong broad plasmon peak is well documented for various Au-NPs with sizes between 2 and 100 nm (Henglein, 1993). Balasubramanian et al. (2020) illustrated that the spherical Au-NPs exhibited the SPR peak at approximately 525–555 nm, which was attributed to the purity and small size of produced Au-NPs. The shape of the resonance peak differs according to the size and nature of Au-NPs (Nellore et al., 2012). Sharp absorbance peaks represent small and uniform-sized NPs; broad absorbance peaks, on the other hand, indicate the larger size distribution or aggregation of NPs (Bakshi et al., 2008). The conduction electrons found on the surface of Au-NPs vibrate in response to a definite wavelength of light resulting in the formation of various brilliant colors. These vibrations generate bright colors based on the shape and size of Au-NPs (AL-Rubaye et al., 2020). The pure crystalline nature of the biosynthesized macroalgae-based Au-NPs was

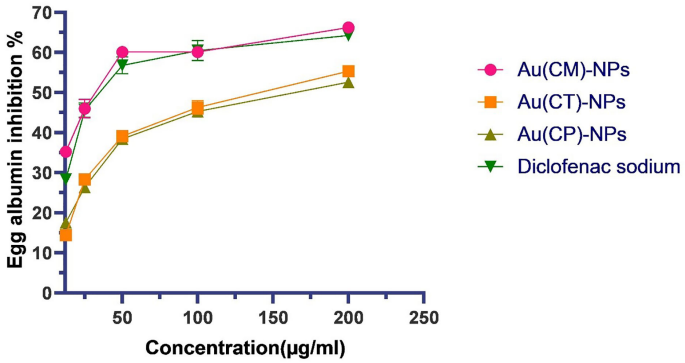

FIGURE 9
Protein denaturation (fresh egg albumin) activity of Au-NPs biosynthesized using macroalgae extracts of *C. myrica* Au(CM)-NPs, *C. trinodis* Au (CT)-NPs, *C. prolifera* Au(CP)-NPs and diclofenac sodium. Values refer to mean± SE.

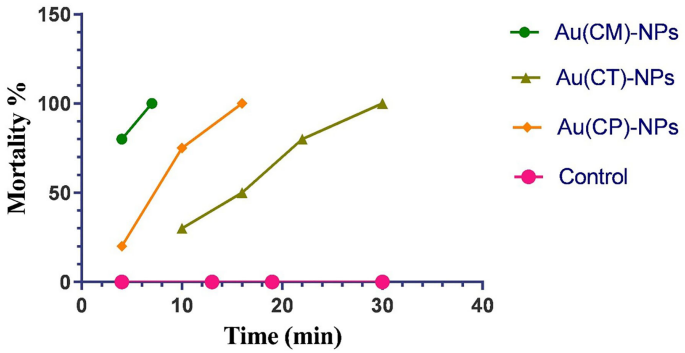

FIGURE 10
Cercaricidal activity of Au-NPs biosynthesized using extracts of macroalgae *C. myrica* Au(CM)-NPs, *C. trinodis* Au(CT)-NPs, and *C. prolifera* Au (CP)-NPs against *S. mansoni* cercariae.

confirmed by XRD analysis through the formation of intense diffraction peaks characterized of Au-NPs, in addition to many additional peaks that attributed to the fact that the other crystalline biomolecules exist in the macroalgal ethanolic extracts (Balasubramanian et al., 2020). XRD patterns show that the degree of crystallinity *of C. trinodis*–based Au-NPs is higher than those of *C. myrica* and *C. prolifera*, which is indicated by the higher diffraction intensity. FT-IR spectroscopy analysis revealed the presence of various secondary metabolites with different functional groups such as hydroxyl and carbonyl groups, possibly aromatic alcohols and amines in the ethanolic extracts of studied macroalgal species, which possibly perform the reduction, capping, and stabilizing of Au-NPs. This result agreed with Algotiml et al. (2022) who reported that the aromatics, amines, or alkanes that exist in the chemical structures of macroalgae could be used as reducing and stabilizing agents for Au-NP biosynthesis. Tao (2018) also reported that proteins might be mainly responsible for capping and stabilizing Au-NPs in the medium, owing to the carbonyl group of amino acids and peptides. Kayalvizhi et al. (2014) compared the production and antimicrobial activity of Ag-NPs and Au-NPs using the extracts of two brown seaweeds (*Padina tetrastromatica* and *Turbinaria ornata*) and stated that Ag-NPs and Au-NPs seem to be related to hydroxyl and carbonyl groups. Similar results were recorded by Rajathi et al. (2012) who studied Au-NP biosynthesis by brown alga biomass (*Stoechospermum marginatum*) and revealed that the reduction of AuCl could be attributed to hydroxyl groups in the diterpenoids of the brown alga. The TEM image of macroalgae-based Au-NPs showed the formation of mostly spherical shapes for *C. myrica*– and *C. trinodis*– based Au-NPs but different shapes (spherical, hexagonal, and triangular) for the Au-NPs of *C. prolifera*. The average size of the produced Au-NPs ranges from 12.6 to 15.5 nm. Even after 30 days of incubation, the Au-NP solution kept a hydrosol without any aggregation or precipitation; this proved that the produced Au-NPs were dispersed well within the solution (Kayalvizhi et al., 2014). Similar results were obtained

by Chaudhary et al. (2020) who investigated the biosynthesis of Au-NPs using red macroalgae, *Lemanea fluviatilis*, and revealed the production of polydispersed crystalline Au-NPs with a diameter of 5.9 nm and González-Ballesteros et al. (2017) who evaluated the production of spherical, stable, polycrystalline Au-NPs with a size of 8.4 nm from the extract of brown seaweed *C. baccata*. Negatively charged NPs tend to give higher stability and avoid particle aggregation, leading to more stable NPs (Babu et al., 2020). Ramakrishna et al. (2016) stated that the high negative potential value revealed the existence of negatively charged compounds in the extract, which provides electrostatic stability to the created Au-NPs.

The marine macroalgae extract presents unlimited opportunities to improve new drugs to combat human pathogenic bacteria owing to the abundance of outstanding bioactive secondary metabolites. Recently, several investigations evaluated the antimicrobial activity of the Au-NPs using many macroalgal species (Rajathi et al., 2012; Naveena and Prakash, 2013; González-Ballesteros et al., 2017; Manikandakrishnan et al., 2019). Strong antibacterial activity against *E. coli* (inhibition zones 22 and 19 mm) was recorded by *C. myrica*– and *C. trinods*–based Au-NPs, respectively, followed by inhibition zones (20.5 and 18 mm) recorded by *C. trinodis*– and *C. myrica*–based Au-NPs, respectively, against *S. aureus*, while the ethanolic extracts of the three macroalgae have no effect on the growth of tested bacteria and fungi. This result proved the validation of the created Au-NPs as a strong antimicrobial agent. Differences in the effect of Au-NPs against tested microorganisms may be attributed to various interactions of Au-NPs with the tested microorganisms as well as the susceptibility of the organism (Aboelfetoh et al., 2017). *E. coli*, followed by *S. aureus*, were found to be the most sensitive toward all biosynthesized Au-NPs using the extracts of studied macroalgae. In general, the Au-NPs of *C. trinodis* followed by the Au-NPs of *C. myrica* presented the best antimicrobial activity compared with the Au-NPs of *C. prolifera*, which recorded the least effect. The results of the current study are in agreement with Rajeshkumar et al. (2013), which recorded that the fabricated Au-NPs using brown macroalgae, *T. conoides*, have antibacterial activity against *Streptococcus* sp., *Bacillus subtilis*, and *Klebsiella pneumonia*. Babu et al. (2020) investigated the biosynthesis of pharmaceutically active Au-NPs using the red macroalgae *Acanthophora spicifera* (As-Au-NPs). As-Au-NPs proved antibacterial activity against *Vibrio harveyi* more than against *S. aureus*. Naveena and Prakash (2013) evaluated the biological synthesis of Au-NPs using the marine alga *Gracilaria corticata* and recorded their potency as an antimicrobial and antioxidant agent. Manikandakrishnan et al. (2019) described the green synthesis of Au-NPs from C. *racemosa* and reported the higher antibacterial activity of the produced Au-NPs against *Aeromonas veronii* than *Streptococcus agalactiae*. The antibacterial activity of Au-NPs may be attributed to the formation of holes in the bacterial cell wall, which leads to cell death due to the loss of cell contents. In addition, Au-NPs can inhibit multidrug-resistant pathogens by adhering to bacterial DNA and blocking the uncoiling of DNA during transcription (Arafa et al., 2018; Sathiyaraj et al., 2021). Moreover, Au-NPs may cause a huge loss of intracellular potassium (Abdel-Raouf et al., 2017). Rónavári et al. (2021) suggested that Au-NPs may destroy the cell membrane potential or inhibit the binding of tRNA to the small subunit of the ribosome; as a result, protein synthesis is hampered. Hu et al. (2020) attributed the antibacterial effect to their high cell affinity, where Au-NPs are simply absorbed by immune cells, allowing accurate transport to the infected tissue to inhibit and destroy pathogenic microbes. Salleh et al. (2020) reported that the activity of ATP synthase is disturbed in the presence of Au-NPs, which ultimately cause cellular ATP deficiency. Abdel-Raouf et al. (2017) proposed that the thiol groups of protein (respiratory enzyme) may be the molecular targets for the Au-NPs. Furthermore, the phospholipid layer in the plasma membrane of the bacteria may be the site of action for the Au-NPs. A different mechanism was suggested by Li et al. (2014) who recorded that the synthesized Au-NPs have the potential to interact with Gram-negative and Gram-positive bacteria, forming aggregation patterns that lead to microbial cell lysis. Au-NPs are significantly biocompatible and have developed resistance slowly across generations, making them a prospective solution for combating multidrug-resistant diseases (Tao, 2018). The increasing drug resistance of fungal strains requires discovering novel drugs for improved fungal disease treatment. *C. trinodis* exhibited the highest antifungal effect against *C. albicans*. This results in agreement with Wani and Ahmad (2013) and Yu et al. (2016), who revealed that the pathogenic fungi *Candida* is sensitive to Au-NPs, which can stop the fungal growth and destroy *C. albicans*. Biosynthesized Au-NPs using tested macroalgae were highly effective as an antibacterial agent than antifungal. Similar results were recorded by Kayalvizhi et al. (2014) with biosynthesized silver and Au-NPs by two species of brown macroalgae (*P. tetrastromatica* and *T. ornata*). Roy et al. (2019) proved the high antifungal effects of Au-NPs, and their study indicated that the main factors determining fungicidal activity are the size, shape, and concentration of Au-NPs. Algotiml et al. (2022) reported strong antifungal activity against dermatophyte fungi and moderate effects against pathogenic Gram-positive and Gram-negative bacteria of Au-NPs synthesized from three seaweeds *Ulva rigida*, *C. myrica*, and *G. foliifera*.

The *in vitro* anti-inflammatory activity of macroalgae-based Au-NPs was studied using the inhibition of egg albumin denaturation. The denaturation of cellular proteins is a well-documented cause of inflammatory reactions. The current macroalgae-based Au-NPs have exhibited good inhibitory potential on protein denaturation, which can be explained by their ability to stabilize the tertiary and quaternary structure of proteins. These findings are similar to Azeem et al. (2022) and more ameliorated than those of Mani et al. (2015) and Prabakaran and Mani (2019).

The current study showed that Au-NPs have significant biocidal activity against *S. mansoni* cercariae. Au-NPs lead to the sinking of the cercariae, followed by their death. Many

previous studies have demonstrated the antiparasitic role of Au-NPs against many other parasitic species. They have a decreased population growth in the promastigote stage of *Leishmania brasiliensis* (Barboza-Filho et al., 2012). They are also toxic to *Plasmodium* and *Cryptosporidium* (Karthik et al., 2013; Joob and Wiwanitkit, 2014). In addition, they have larvicidal properties against a mosquito vector of malaria (Navarro et al., 1997; Navarro et al., 2004). Furthermore, Au-NPs showed promising protective roles against mice infected with *S. mansoni* (Dkhil et al., 2019). Overall, the biosynthesized macroalgae-based Au-NPs evaluated in this study can offer a good alternative to produce antimicrobial agents against multidrug-resistant pathogenic bacteria and fungi. Furthermore, they possess strong inhibitory potential on protein denaturation and antiparasitic activity against parasites that cause human diseases such as *S. mansoni.*

Conclusion

The current study investigated the biosynthesis of eco-friendly Au-NPs from the macroalgal extracts of three seaweeds *C. myrica, C. trinodis*, and *C. prolifera*. The obtained results revealed the biosynthesis of highly stable Au-NPs with an average size from 12.6 to 15.5 nm with pure crystalline nature. These findings confirm that macroalgal extract components can serve as a reducing, capping, and stabilizing agent for Au-NP fabrication. Biosynthesized Au-NPs were proven to have significant antibacterial and antifungal activities against many pathogenic bacteria and fungi strains, particularly *C. myrica*– and *C. trinodis*–based Au-NPs. Furthermore, the produced Au-NPs exhibited strong inhibitory potential on protein denaturation and a schistolarvicidal effect against *S. mansoni* cercariae.

Data availability statement

The original contributions presented in the study are included in the article/supplementary material. Further inquiries can be directed to the corresponding author.

Author contributions

KE: Conception or design of the work, data collection, data analysis, and interpreting and drafting the article; HA-T: data collection and data analysis and interpretation; MK: data collection and drafting the article; HS; OH, MA, and NA-R: Equally contributed to the critical revision of the article and the final approval of the version to be published.

Funding

Princess Nourah bint Abdulrahman University Researchers Supporting Project number (PNURSP2022R83), Princess Nourah bint Abdulrahman University, Riyadh, Saudi Arabia.

Acknowledgments

Princess Nourah bint Abdulrahman University Researchers Supporting Project number (PNURSP2022R83), Princess Nourah bint Abdulrahman University, Riyadh, Saudi Arabia.

Conflict of interest

The authors declare that the research was conducted in the absence of any commercial or financial relationships that could be construed as a potential conflict of interest.

Publisher's note

References

Abdel-Raouf, N., Al-Enazi, N. M., Ibraheem, I. B. M., Alharbi, R. M., and Alkhulaifi, M. M. (2017). Biosynthesis of silver nanoparticles by using of the marine brown alga *Padina pavonia* and their characterization. *Saudi J. Biol. Sci.* 26 (6), 1207–1215. doi: 10.1016/j.sjbs.2018.01.007

Aboelfetoh, E. F., El-Shenody, R. A., and Ghobara, M. M. (2017). Eco-friendly synthesis of silver nanoparticles using green algae (*Caulerpa serrulata*): reaction optimization, catalytic and antibacterial activities. *Environ. Monit. Assess.* 189 (7), 1–15. doi: 10.1007/s10661-017-6033-0

Adekiya, T. A., Kappo, A. P., and Okosun, K. O. (2017). Temperature and rainfall impact on schistosomiasis. *Glob. J. Pure Appl. Math.* 13, 8453–8469.

Ahmed, S. F., Mofijur, M., Rafa, N., Chowdhury, A. T., Chowdhury, S., Nahrin, M., et al. (2022). Green approaches in synthesising nanomaterials for environmental nanobioremediation: Technological advancements, applications, benefits and challenges. *Environ. Res.* 204, 111967. doi: 10.1016/j.envres.2021.111967

Algotiml, R., Gab-alla, A., Seoudi, R., Abulreesh, H. H., Ahmad, I., and Elbanna, K. (2022). Anticancer and antimicrobial activity of red Sea seaweeds extracts-mediated gold nanoparticles. *J. Pure Appl. Microbiol.* 16 (1), 207–226. doi: 10.22207/JPAM.16.1.11

Alipour, H. J., Rezaei, M., Shabanpour, B., and Tabarsa, M. (2018). Effects of sulfated polysaccharides from green alga ulva intestinalis on physicochemical

properties and microstructure of silver carp surimi *Food. Hydrocoll.* 74, 87–96. doi: 10.1016/j.foodhyd.2017.07.038

AL-Rubaye, H. I., Al-Abodi, E. E., and Yousif, E. I. (2020). Green chemistry synthesis of modified silver nanoparticles. *Phys. Conf. Ser.* 1664 (1), 1–26. doi: 10.1088/1742-6596/1664/1/012080

Amin, B. H., Ahmed, H. Y., El Gazzar, E. M., and Badawy, M. M. (2021). Enhancement the mycosynthesis of selenium nanoparticles by using gamma radiation. *Dose-Response* 19 (4). doi: 10.1177/15593258211059323

Arafa, M. G., El-Kased, R. F., and Elmazar, M. M. (2018). Thermoresponsive gels containing gold nanoparticles as smart antibacterial and wound healing agents. *Sci. Rep.* 8 (1), 1–16. doi: 10.1038/s41598-018-31895-4

Arévalo-Gallegos, A., Garcia-Perez, J. S., Carrillo-Nieves, D., Ramirez-Mendoza, R. A., Iqbal, H. M., and Parra-Saldivar, R. (2018). Botryococcus braunii as a bioreactor for the production of nanoparticles with antimicrobial potentialities. *Int. J. Nanomed.* 13, 5591. doi: 10.2147/IJN.S174205

Azeem, M. N. A., Ahmed, O. M., Shaban, M., and Elsayed, K. N. (2022). *In vitro* antioxidant, anticancer, anti-inflammatory, anti-diabetic and anti-Alzheimer potentials of innovative macroalgae bio-capped silver nanoparticles. *Environ. Sci. pollut. Res.*, 1–18. doi: 10.1007/s11356-022-20039-x

Babu, B., Palanisamy, S., Vinosha, M., Anjali, R., Kumar, P., Pandi, B., et al. (2020). Bioengineered gold nanoparticles from marine seaweed acanthophora spicifera for pharmaceutical uses: antioxidant, antibacterial, and anticancer activities. *Bioprocess Biosyst. Eng.* 43 (12), 2231–2242. doi: 10.1007/s00449-020-02408-3

Bafana, A. (2013). Characterization and optimization of production of exopolysaccharide from chlamydomonas reinhardtii. *Carbohydr. Polym.* 95 (2), 746–752. doi: 10.1016/j.carbpol.2013.02.016

Bakshi, M. S., Sachar, S., Kaur, G., Bhandari, P., Kaur, G., Biesinger, M. C., et al. (2008). Dependence of crystal growth of gold nanoparticles on the capping behavior of surfactant at ambient conditions. *Cryst. Growth Des.* 8 (5), 1713–1719. doi: 10.1021/cg8000043

Balasubramanian, S., Kala, S. M. J., and Pushparaj, T. L. (2020). Biogenic synthesis of gold nanoparticles using *Jasminum auriculatum* leaf extract and their catalytic, antimicrobial and anticancer activities. *J. Drug Deliv. Sci. Tec.* 57, 101620. doi: 10.1016/j.jddst.2020.101620

Barboza-Filho, C. G., Cabrera, F. C., and Dos Santos, R. J. (2012). The influence of natural rubber/Au nanoparticle membranes on the physiology of *Leishmania brasiliensis*. *Experimen. Parasitol* 130, 152–158. doi: 10.1016/j.exppara.2011.10.015

Barry, M. A., Simon, G. G., Mistry, N., and Hotez, P. J. (2013). Global trends in neglected tropical disease control and elimination: Impact on child health. *Arch. Dis. Childh. Lond.* 98, 635–641. doi: 10.1136/archdischild-2012-302338

Borse, V. B., Konwar, A. N., Jayant, R. D., and Patil, P. O. (2020). Perspectives of characterization and bioconjugation of gold nanoparticles and their application in lateral flow immunosensing. *Drug Deliv. Transl. Res.* 10 (4), 878–902. doi: 10.1007/s13346-020-00771-y

Chandini, S. K., Ganesan, P., and Bhaskar, N. (2008). *In vitro* antioxidant activities of three selected brown seaweeds of India. *Food. Chem.* 107, 707–713. doi: 10.1016/j.foodchem.2007.08.081

Chapman, V. J., and Chapman, D. J. (1980). *Seaweeds and their uses. 3rd ed.* Vol. 96 (London, New York), 234–237.

Chaudhary, R., Nawaz, K., Khan, A. K., Hano, C., Abbasi, B. H., and Anjum, S. (2020). An overview of the algae-mediated biosynthesis of nanoparticles and their biomedical applications. *Biomolecules* 10 (11) 1498. doi: 10.3390/biom10111498

Colley, D. G., Bustinduy, A. L., Secor, W. E., and King, C. H. (2014). Human schistosomiasis. *Lancet* 383, 2253–2264. doi: 10.1016/S0140-6736(13)61949-2

Devi, G. K., Manivannan, K., Thirumaran, G., Rajathi, F. A. A., and Anantharaman, P. (2011). *In vitro* antioxidant activities of selected seaweeds from southeast coast of India. *Asian Pac. J. Trop. Med.* 4 (3), 205–211. doi: 10.1016/S1995-7645(11)60070-9

Dkhil, M. A., Khalil, M. F., Diab, M. S., Bauomy, A. A., Santourlidis, S., Al-Shaebi, E. M., et al. (2019). Evaluation of nanoselenium and nanogold activities against murine intestinal schistosomiasis. *Saudi J. Biol. Sci.* 26, 1468–1472. doi: 10.1016/j.sjbs.2018.02.008

Eissa, M. M., El Bardicy, S., and Tadros, M. (2011). Bioactivity of miltefosine against aquatic stages of *Schistosoma mansoni*, *Schistosoma haematobium* and their snail hosts, supported by scanning electron microscopy. *Parasites Vectors* 4, 1–11. doi: 10.1186/1756-3305-4-73

Elfaki, T. M., Hamad, M. N., Zarrug, E., Mohammed, H. O., Mohammed, S. H., Ahmad, R. A., et al. (2020). Prevalence of schistosomiasis among school aged children in altakamol area_Kha toum state_Sudan. *J. Microbiol. Exp.* 8, 167–169.

Elias, G., and Rao, M. N. (1988). Inhibition of albumin denaturation and anti-unflammatory activity of dehydrozingerone and its analogs. *Indian. J. Exp. Biol.* 26 (10), 540–542.

Elsayed, K. N., Mohamed, A. M., Noke, A., and Klöck, G. (2017a). Microalgae as an alternative source for biodiesel and biogas production–A mini review. *Nat. Sci.* 15 (12), 1–16. doi: 10.7537/marsnsj151217.01

Elsayed, K. N., Kolesnikova, T. A., Noke, A., and Klöck, G. (2017b). Imaging the accumulated intracellular microalgal lipids as a response to temperature stress. *Biotech* 7 (1), 1–8. doi: 10.1007/s13205-017-0677-x

El-Kassas, H. Y., and Ghobrial, M. G. (2017). Biosynthesis of metal nanoparticles using three marine plant species: anti-algal efficiencies against "*Oscillatoria simplicissima*". *Environ. Sci. pollut. Res.* 24, 7837–7849. doi: 10.1007/s11356-017-8362-5

Fathy, W., Elsayed, K., Essawy, E., Tawfik, E., Zaki, A., Abdelhameed, M. S., et al (2020). Biosynthesis of Silver Nanoparticles from Synechocystis sp to be Used as a Flocculant Agent with Different Microalgae Strains. *Current Nanomaterials* 5 (2), 175–87. doi: 10.2174/2468187310999200605161200

Fathy, W., Essawy, E., Tawfik, E., Khedr, M., Abdelhameed, M. S., Hammouda, O., et al (2021). Recombinant overexpression of the Escherichia coli acetyl-CoA carboxylase gene in Synechocystis sp. boosts lipid production. *Journal of Basic Microbiology* 61 (4), 330–338. doi: 10.1002/jobm.202000656

Faradilla, F., Nikmah, F., Putri, A. D., Agustin, G. A., Nurkaromah, L., Febrianti, M. W., et al. (2022). Macroalgae diversity at porok beach, gunungkidul, yogyakarta, Indonesia. *J. Agric. Appl. Biol.* 3 (1), 50–61. doi: 10.11594/jaab.03.01.06

Fawcett, D., Verduin, J. J., Shah, M., Sharma, S. B., and Poinern, G. E. J. (2017). A review of current research into the biogenic synthesis of metal and metal oxide nanoparticles *via* marine algae and seagrasses. *J. Nanosci.* 2017, 1–15. doi: 10.1155/2017/8013850

Fernández, P. V., Ciancia, M., and Estévez, J. M. (2011). Cell wall variability in the green seaweed *Codium vermilara* (bryopsidales chlorophyta) from the Argentine coast. *J. Phycol.* 47, 802–810. doi: 10.1111/j.1529-8817.2011.01006.x

Ghiyasiyan-Arani, M., Salavati-Niasari, M., and Naseh, S. (2017). Enhanced photodegradation of dye in waste water using iron vanadate nanocomposite; ultrasound-assisted preparation and characterization. *Ultrasonics Sonochemistry* 39, 494–503. doi: 10.1016/j.ultsonch.2017.05.025

Gholami, T., Salavati-Niasari, M., and Varshoy, S. (2017). Electrochemical hydrogen storage capacity and optical properties of NiAl2O4/NiO nanocomposite synthesized by green method. *Int. J. hydrogen Energy* 42 (8), 5235–5245. doi: 10.1016/j.ijhydene.2016.10.132

Ghosh, S., Patil, S., Ahire, M., Kitture, R., Gurav, D. D., Jabgunde, A. M., et al. (2012). Gnidia glauca flower extract mediated synthesis of gold nanoparticles and evaluation of its chemocatalytic potential. *J. Nanobiotechnol.* 10 (1), 1–9. doi: 10.1186/1477-3155-10-17

Gomathy, J., Jayalakshmi, L., Jayanthi, J., and Ragunathan, M. G. (2021). An in Vitro Study on the Antimicrobial Activity and Antioxidant Activities of the Extract of A Seaweed, Enteromorpha Intestinalis Against Certain Pathogens. doi: 10.21203/rs.3.rs-1116593/v1

González-Ballesteros, N., Prado-López, S., Rodríguez-González, J., Lastra, M., and Rodríguez-Argüelles, M. (2017). Green synthesis of gold nanoparticles using brown algae *Cystoseira baccata*: its activity in colon cancer cells. *Colloids Surf. B: Biointerfaces* 153, 190–198. doi: 10.1016/j.colsurfb.2017.02.020

González-Ballesteros, N., Rodríguez-Argüelles, M. C., Lastra-Valdor, M., González-Mediero, G., Rey-Cao, S., Grimaldi, M., et al. (2020). Synthesis of silver and gold nanoparticles by sargassum muticum biomolecules and evaluation of their antioxidant activity and antibacterial properties. *J. Nanostruct. Chem.* 10, 317–330. doi: 10.1007/s40097-020-00352-y

Henglein, A. (1993). Physicochemical properties of small metal particles in solution: "microelectrode" reactions, chemisorption, composite metal particles, and the atom-to-metal transition. *J. Phys. Chem.* 97 (21), 5457–5471. doi: 10.1021/j100123a004

Heydariyan, Z., Monsef, R., and Salavati-Niasari, M. (2022). Insights into impacts of Co3O4-CeO2 nanocomposites on the electrochemical hydrogen storage performance of g-C3N4: Pechini preparation, structural design and comparative study. *J. Alloys Compounds* 924, 166564. doi: 10.1016/j.jallcom.2022.166564

Hotez, P. J., Alvarado, M., Basáñez, M., Bolliger, I., Bourne, R., Boussinesq, M., et al. (2014). The global burden of disease study 2010: Interpretation and implications for the neglected tropical diseases. *PloS Negl. Trop. Dis.* 8, e2865. doi: 10.1371/journal.pntd.0002865

Hu, X., Zhang, Y., Ding, T., Liu, J., and Zhao, H. (2020). Multifunctional gold nanoparticles: a novel nanomaterial for various medical applications and biological activities. *Front. Bioeng. Biotechnol.* 8. doi: 10.3389/fbioe.2020.00990

Hussein, M., Zaki, A., Abdel-Raouf, N., Alsamhary, K., Fathy, W., Abdelhameed, M., et al (2022). Flocculation of microalgae using calcium oxide nanoparticles; process optimization and characterization. *Int. Aquat. Res.* 14 (1), 63–70. doi: / 10.22034/IAR.2022.1943339.1206

Ibrahim, A. M., and Abdel-Tawab, H. (2020). *Cystoseira barbata* marine algae have a molluscicidal activity against *Biomphalaria alexandrina* snails supported by

scanning electron microscopy, hematological and histopathological alterations, and larvicidal activity against the infective stages of *Schistosoma mansoni*. *Biologia* 75, 1945–1954. doi: 10.2478/s11756-020-00457-3

Joob, B., and Wiwanitkit, V. (2014). "Effect of gold nanoparticle solution on cryptosporidium oocyst: The world first report," in *Annals of tropical medicine and public health*, vol. 7. , 192–193. doi: 10.4103/1755-6783.149506

Karthik, L., Kumar, G., Keswani, T., Bhattacharyya, A., Reddy, B. P., and Rao, K. B. (2013). Marine actinobacterial mediated gold nanoparticles synthesis and their antimalarial activity. *Nanomed.: Nanotechnol. Biol. Med.* 9 (7), 951–960. doi: 10.1016/j.nano.2013.02.002

Kayalvizhi, K., Asmathunisha, N., Subramanian, V., and Kathiresan, K. (2014). Purification of silver and gold nanoparticles from two species of brown seaweeds (*Padina tetrastromatica* and *Turbinaria ornata*). *J. Med. Plants. Stud.* 2 (4), 32–37.

Kayalvizhi, K., Subramanian, N. V., Boopathy, N. S., and Kathiresan, K. (2014). Antioxidant properties of brown seaweeds *Turbinaria ornata (Turner) j. agardh* 1848 and *Padina tetrastromatica (Hauck)*. *J. Biotechnol. Sci.* 2 (1), 29–37.

Khandelia, R., Bhandari, S., Pan, U. N., Ghosh, S. S., and Chattopadhyay, A. (2015). Gold nanocluster embedded albumin nanoparticles for two- photon imaging of cancer cells accompanying drug delivery. *Small* 11 (33), 4075–4081. doi: 10.1002/smll.201500216

Khanna, P., Kaur, A., and Goyal, D. (2019). Algae-based metallic nanoparticles: Synthesis, characterization and applications. *J. Microbial. Meth.* 163, 105656. doi: 10.1016/j.mimet.2019.105656

Khan, T., Ullah, N., Khan, M. A., Mashwani, Z. R., and Nadhman, A. (2019). Plant-based gold nanoparticles: a comprehensive review of the decade-long research on synthesis, mechanistic aspects and diverse applications. *Adv. Colloid. Int. Sci.* 272, 102017. doi: 10.1016/j.cis.2019.102017

Li, X., Robinson, S. M., Gupta, A., Saha, K., Jiang, Z., Moyano, D. F., et al. (2014). Functional gold nanoparticles as potent antimicrobial agents against multi-drug-resistant bacteria. *ACS Nano.* 8 (10), 10682–10686. doi: 10.1021/nn5042625

Manikandakrishnan, M., Palanisamy, S., Vinosha, M., Kalanjiaraja, B., Mohandoss, S., Manikandan, R., et al. (2019). Facile green route synthesis of gold nanoparticles using *Caulerpa racemosa* for biomedical applications. *J. Drug Deliv. Sci. Tec.* 54, 101345. doi: 10.1016/j.jddst.2019.101345

Mani, A. K., Seethalakshmi, S., and Gopal, V. (2015). Evaluation of *in-vitro* anti-inflammatory activity of silver nanoparticles synthesised using *piper nigrum* extract. *J. Nanomed. Nanotechnol.* 6 (2), 1.

Mayer, A. M.S., Rodriguez, A. D., Taglialatela-Scafati, O., and Fusetani, N. (2013). Marine pharmacolgy in 2009- 2011: marine compounds with antibacterial, antidiabetic, antifungal, anti-inflammatory, antiprotozoal, antituberculosis, and antiviral activities; affecting the immune and nervous systems, and other miscellaneous mechanisms of action. *Mar. Drugs* 11, 2510–73. doi: 10.3390/md11072510

Menon, S., Rajeshkumar, S., and Kumar, V. (2017). A review on biogenic synthesis of gold nanoparticles, characterization, and its applications. *Resource-Efficient Technol.* 3 (4), 516–527. doi: 10.1016/j.reffit.2017.08.002

Mir, N., and Salavati-Niasari, M. (2013). Preparation of TiO2 nanoparticles by using tripodal tetraamine ligands as complexing agent *via* two-step sol–gel method and their application in dye-sensitized solar cells. *Materials Res. Bull.* 48 (4), 1660–1667. doi: 10.1016/j.materresbull.2013.01.006

Monsef, R., Ghiyasiyan-Arani, M., and Salavati-Niasari, M. (2018). Application of ultrasound-aided method for the synthesis of NdVO 4 nano-photocatalyst and investigation of eliminate dye in contaminant water. *Ultrasonics Sonochem.* 42, 201–211. doi: 10.1016/j.ultsonch.2017.11.025

Monsef, R., and Salavati-Niasari, M. (2023). Architecturally robust tubular nano-clay grafted Li0. 9Ni0.5Co0. 5O2-x/LiFeO2 nanocomposites: New implications for electrochemical hydrogen storage. *Fuel* 332, 126015.

Moustafa, M. A., Mossalem, H. S., Sarhan, R. M., Abdel-Rahman, A. A., and Hassan, E. M. (2018). The potential effects of silver and gold nanoparticles as molluscicides and cercaricides on Schistosoma mansoni. *Parasitology Res* 117 (12), 3867–3880. doi: 10.1007/s00436-018-6093-2

Navarro, M., Pérez, H., and Sánchez-Delgado, R. A. (1997). Toward a novel metal-based chemotherapy against tropical diseases. 3. synthesis and antimalarial activity *in vitro* and *in vivo* of the new gold– chloroquine complex [Au (PPh3) (CQ)] PF6. *J. Med. Chem.* 40 (12), 1937–1939. doi: 10.1021/jm9607358

Navarro, M., Vásquez, F., Sánchez-Delgado, R. A., Pérez, H., Sinou, V., and Schrével, J. (2004). Toward a novel metal-based chemotherapy against tropical diseases. 7. synthesis and *in vitro* antimalarial activity of new goldchloroquine complexes. *J. Med. Chem.* 47 (21), 5204–5209. doi: 10.1021/jm049792o

Naveena, B. E., and Prakash, S. (2013). Biological synthesis of gold nanoparticles using marine algae *Gracilaria corticata* and its application as a potent antimicrobial and antioxidant agent. *Asian. J. Pharm. Clin. Res.* 6 (2), 179–182.

Nellore, J., Pauline, P. C., and Amarnath, K. (2012). Biogenic synthesis by *Sphearanthus amaranthoids*; towards the efficient production of the biocompatible gold nanoparticles. *Dig. J. Nanomater. Biostruct.* 7, 123–133.

Osman, M. E., Abo-Shady, A. M., Elshobary, M. E., El-Ghafar, A., Mahasen, O., and Abomohra, A. E. F. (2020). Screening of seaweeds for sustainable biofuel recovery through sequential biodiesel and bioethanol production. *Environ. Sci. pollut. Res.* 27 (26), 32481–32493. doi: 10.1007/s11356-020-09534-1

Öztürk, B. Y. (2019). Intracellular and extracellular green synthesis of silver nanoparticles using desmodesmus sp.: their antibacterial and antifungal effects. *Caryologia* 72 (1), 29–43. doi: 10.13128/cayologia-246

Panahi-Kalamuei, M., Alizadeh, S., Mousavi-Kamazani, M., and Salavati-Niasari, M. (2015). Synthesis and characterization of CeO2 nanoparticles *via* hydrothermal route. *J. Ind. Eng. Chem.* 21, 1301–1305. doi: 10.1016/j.jiec.2014.05.046

Pantidos, N., and Horsfall, L. E. (2014). Biological synthesis of metallic nanoparticles by bacteria, fungi and plants. *J. Nanomed. Nanotechnol.* 5 (5), 1. doi: 10.4172/2157-7439.1000233

Patterson, A. L. (1939). The scherrer formula for X-ray particle size determination. physical review. *Am. Phys. Soc.* 56 (10), 978–982. doi: 10.1103/physrev.56.978

Paulkumar, K., Gnanajobitha, G., Vanaja, M., Pavunraj, M., and Annadurai, G. (2017). Green synthesis of silver nanoparticle and silver based chitosan bionanocomposite using stem extract of saccharum officinarum and assessment of its antibacterial activity. *Adv. Nat. Sci-Nanosci.* 8 (3), 035019. doi: 10.1088/2043-6254/aa7232

Pereira, L. (2018). Seaweeds as source of bioactive substances and skin care therapy cosmeceuticals, algotheraphy, and thalassotherapy. *Cosmetics* 5, 4, 68. doi: 10.3390/cosmetics5040068

Prabakaran, A. S., and Mani, N. (2019). Anti-inflammatory activity of silver nanoparticles synthesized from *Eichhornia crassipes*: An *in vitro* study. *J. Pharmacogn. Phytochem.* 8 (4), 2556–2558.

Pulakkat, S., and Patravale, V. B. (2020). "Marine resources for biosynthesis and surface modification of anticancer nanoparticles," in *Green synthesis of nanoparticles: Applications and prospects* (Singapore: Springer), 141–161.

Purohit, J., Chattopadhyay, A., and Singh, N. K. (2019). "Green synthesis of microbial nanoparticle: approaches to application," in *Microbial nanobionics* (Cham: Springer), 35–60.

Rajathi, F. A. A., Parthiban, C., Kumar, V. G., and Anantharaman, P. (2012). Biosynthesis of antibacterial gold nanoparticles using brown alga, stoechospermum marginatum (kützing). *Spectrochimica acta part a. Mol. Biomol. Spectrosc. Mol. Biomolecular Spectrosc.* 99, 166–173. doi: 10.1016/j.saa.2012.08.081

Rajeshkumar, S., Malarkodi, C., Vanaja, M., Gnanajobitha, G., Paulkumar, K., Kannan, C., et al. (2013). Antibacterial activity of algae mediated synthesis of gold nanoparticles from turbinaria conoides. *Der Pharma Chemica.* 5 (2), 224–229. doi: 10.1186/2193-8865-3-44

Ramakrishna, M., Rajesh Babu, D., Gengan, R. M., Chandra, S., and Nageswara Rao, G. (2016). Green synthesis of gold nanoparticles using marine algae and evaluation of their catalytic activity. *J. Nanostruct. Chem.* 6 (1), 1–13. doi: 10.1007/s40097-015-0173-y

Ramli, A. N. M., Badrulzaman, S. Z. S., Hamid, H. A., and Bhuyar, P. (2021). Antibacterial and antioxidative activity of the essential oil and seed extracts of artocarpus heterophyllus for effective shelf-life enhancement of stored meat. *J. Food. Process. Preserv.* 45 (1), e14993. doi: 10.1111/jfpp.14993

Robert, E. L. (1989). *Phycology. 2nd ed.* Vol. 115 (Cambridge University press), 3–41.

Rónavári, A., Igaz, N., Adamecz, D. I., Szerencsés, B., Molnar, C., Kónya, Z., et al. (2021). Green silver and gold nanoparticles: Biological synthesis approaches and potentials for biomedical applications. *Molecules* 26 (4), 844. doi: 10.3390/molecules26040844

Roy, S., Mondal, A., Yadav, V., Sarkar, A., Banerjee, R., Sanpui, P, et al. (2019). Mechanistic insight into the antibacterial activity of chitosan exfoliated MoS2 nanosheets: membrane damage, metabolic inactivation, and oxidative stress. ACS. *Appl. Bio. Mater.* 2 (7), 2738–2755. doi: 10.1021/acsabm.9b00124

Sahoo, A. K., Banerjee, S., Ghosh., S. S., and Chattopadhyay, A. (2014). Simultaneous RGB emitting au nanoclusters in chitosan nanoparticles for anticancer gene theranostics. *ACS. Appl. Mater. Interfaces* 6 (1), 712–724. doi: 10.1021/am4051266

Salavati-Niasari, M., Salemi, P., and Davar, F. (2005). Oxidation of cyclohexene with tert-butylhydroperoxide and hydrogen peroxide catalysted by Cu (II), Ni (II), Co (II) and Mn (II) complexes of n, n′-bis-(α-

methylsalicylidene)-2, 2-dimethylpropane-1, 3-diamine, supported on alumina. *J. Mol. Catalysis A: Chemical.* 238 (1-2), 215–222. doi: 10.1016/j.molcata.2005.05.026

Salem, S. S., and Fouda, A. (2021). Green synthesis of metallic nanoparticles and their prospective biotechnological applications: an overview. *Biol. Trace. Elem. Res.* 199 (1), 344–370. doi: 10.1007/s12011-020-02138-3

Salleh, A., Naomi, R., Utami, N. D., Mohammad, A. W., Mahmoudi, E., Mustafa, N., et al. (2020). The potential of silver nanoparticles for antiviral and antibacterial applications: A mechanism of action. *Nanomaterials* 10 (8), 1566. doi: 10.3390/nano10081566

Sathiyaraj, S., Suriyakala, G., Gandhi, A. D., Babujanarthanam, R., Almaary, K. S., Chen, T. W., et al. (2021). Biosynthesis, characterization, and antibacterial activity of gold nanoparticles. *J. Infection Public Health* 14 (12), 1842–1847. doi: 10.1016/j.jiph.2021.10.007

Shukla, A. K., Upadhyay, A. K., and Singh, L. (2021). "Algae-mediated biological synthesis of nanoparticles: applications and prospects,". Eds. S. K. Mandotra, A. K. Upadhyay and A. S. Ahluwalia *Algae* (Singapore: Springer), 325–338. doi: 10.1007/978-981-15-7518-1_14

Soureshjani, P. T., Shadi, A., and Mohammadsaleh, F. (2021). Algae-mediated route to biogenic cuprous oxide nanoparticles and spindle-like CaCO 3: a comparative study, facile synthesis, and biological properties. *RSC Adv.* 11 (18), 10599–10609. doi: 10.1039/D1RA00187F

Tao, C. (2018). Antimicrobial activity and toxicity of gold nanoparticles: research progress, challenges, and prospects. *Lett. Appl. Microbiol.* 67 (6), 537–543. doi: 10.1111/lam.13082

Usman, A. I., Aziz, A. A., and Noqta, O. A. (2019). Green sonochemical synthesis of gold nanoparticles using palm oil leaves extracts. *Mater. Today Proc.* 7, 803–807. doi: 10.1016/j.matpr.2018.12.078

Wani, I. A., and Ahmad, T. (2013). Size and shape dependent antifungal activity of gold nanoparticles: a case study of candida. *Colloids Surf. B:Biointerfaces* 101, 162–170. doi: 10.1016/j.colsurfb.2012.06.005

Wibowo, K. M., Talib, A., Ani, N. C., Ahmad, N., Muslihati, A., and Rosni, N. M. (2019). "A REVIEW OF GRAPHENE MATERIALS-BASED SENSORS. a REVIEW OF GRAPHENE MATERIALS-BASED SENSORS," in *Current advances in microdevices and nanotechnology series*, vol. 101. .

World Health Organization (2015). *Female genital schistosomiasis: a pocket atlas for clinical health-care professionals (No. WHO/HTM/NTD/2015.4).*

Yassin, M. A., Elgorban, A. M., El-Samawaty, A. E-RM, and Almunqedhi, B. M. (2021). Biosynthesis of silver nanoparticles using *Penicillium verrucosum* and analysis of their antifungal activity. *Saudi J. Biol. Sci.* 28, 2123–2127. doi: 10.1016/j.sjbs.2021.01.063

Yu, Q., Li, J., Zhang, Y., Wang, Y., Liu, L., and Li, M. (2016). Inhibition of gold nanoparticles (AuNPs) on pathogenic biofilm formation and invasion to host cells. *Sci. Rep.* 6 (1), 1–14. doi: 10.1038/srep26667